A framework for detecting stage-discharge hysteresis due to flow unsteadiness: Application to France's national hydrometry network

E. Perret, M. Lang, J. Le Coz

A framework for detecting stage-discharge hysteresis due to flow unsteadiness : application to France's national hydrometry network

E. Perret[1,2*], M. Lang[1], and J. Le Coz[1]

[1]INRAE, UR RiverLy, F-69100, Villeurbanne, France
[2]Compagnie Nationale du Rhône, CNR, Lyon, France
[*]Corresponding author, e-mail: e.perret@cnr.tm.fr

January 12, 2022

Abstract

A generic framework is proposed to evaluate the relative discharge error made when ignoring stage-discharge hysteresis due to transient flow over large gauging station networks. The diagnosis is conducted using the Jones equation, based on a simple hydraulic concept relating discharge to stage and its time-gradient. The main input data used for the method are the flow resistance coefficients, the temporal stage gradients, and the bed slopes. The hysteresis effect is quantified for each gauging station and mapped using the relative discharge error. The method was applied to 2618 gauging stations of France's national hydrometry network using observational data extracted from the national hydrological archive and from Digital Terrain Models. The diagnostic results highly depend on slope estimates used as inputs. Substantial hysteresis effects were found at stations with low bed slope combined with a fast flood regime. The France application shows the difficulty to provide a firm conclusion about stations prone to hysteresis due to the slope data uncertainty. This issue is not specific to France; slope estimates at a country-level is difficult to obtain in many countries. The use of local bed slope estimates is recommended to approach the slopes of the reaches controlling the station flow dynamics.

Keywords: rating curve; hysteresis; diagnosis; unsteady flow.

1 Introduction

Hysteresis in the stage-discharge relations (i.e. rating curves) of gauging stations can be observed during flood events (Rantz, 1982; Muste et al., 2020). Figure 1 is an illustration of the effect of unsteady flows on different flow variables in time and on the stage-discharge relationship compared to the case of uniform steady flows. During the propagation of transient flows, the celerity of the pressure wave (stage) is smaller than the celerity of the velocity wave, hence smaller than the celerity of the discharge wave (Graf and Qu, 2004). In such case, for the same given stage, the discharge during the rising limb is higher than during the falling limb of the event, leading to a non-unique stage-discharge relation. Hysteresis creates a loop in the rating curve, which is more or less wide depending on the geometrical characteristics of the channel and on the type (intensity, gradient) of floods (Lee, 2013). Other phenomena can create looped rating curves, such as variable backwater (i.e. changes in the downstream conditions), or variable roughness (Boyer, 1964; Fenton and Keller, 2001; Mansanarez, 2016). In this study, the focus is on hysteresis induced by unsteady flow only.

In practice, this hysteresis effect is often neglected, partly because it is not captured by the occasional measurements of discharge and stage (a.k.a. gaugings). Indeed, during flood events, gaugings are generally made after the flood peaks, for practical and safety reasons. Thus, the loop induced by the hysteresis phenomenon in the rating curve is often not observed. The evolution of the gauging techniques toward non-intrusive and less dangerous methods, e.g. radar (Welber et al., 2016) and image velocimetry (Dramais et al., 2011), will certainly help to overcome this lack of information in the coming years. Substantial biases in flood prediction can arise if hysteresis is ignored, such as underestimation of discharge during the rising limb of the flood, including the peak discharge, time lag in the overall flood hydrograph and larger uncertainty of the discharge estimations due to the scatter of gauging data around the rating curve (Holmes, 2016; Mansanarez, 2016; Muste et al., 2020).

Numerous methods exist to adjust the rating curves when unsteadiness is significant (cf. Lee, 2013; Dottori et al., 2009, for method reviews). They are usually based on a correction of the standard discharge, estimated with a unique rating curve valid for steady flow conditions, to account for hysteresis and compute the real discharge. Jones (1915) method is the most used by the hydrometric community. It assumes that the flood wave propagates without any attenuation. Based on this kinetic wave approximation, the discharge in unsteady flows can be deduced from the stage and its time-gradient. More general expressions accounting for inertial forces have been proposed and used by Fread (1975); Fenton and Keller (2001); Perumal et al. (2004); Petersen-Overleir (2006); Wolfs and Willems (2014); Mansanarez (2016); Lee and Muste (2017); Muste et al. (2020) for example.

It is important to know where and when hysteresis can occur and how large it is to better evaluate the flood hazard (Lee, 2013; Muste et al., 2020). The main objective of this paper is to propose a diagnostic approach to quantify the risk of hysteresis over a large set of hydrometric stations, typically over an entire national network. The gauging stations prone to hysteresis are identified from the relative discharge error ϵ potentially made when ignoring the hysteresis effect. The parameter ϵ is defined as the relative bias between discharge estimates accounting (Q) or not (Q_0) for flow unsteadiness (Figure 1). It informs about the exposure of gauging stations to hysteresis effect during specific events. The parameter ϵ is similar to the PDIFF parameter introduced by Holmes (2016), which refers to the percent difference of the measured discharge from the discharge estimated using the unique standard rating curve. However, ϵ seems more suitable for massive diagnosis since it is based solely on discharge models and does not depend on available discharge measurements. The diagnosis is intended to massive and large-scale deployment and to overview the areas influenced by hysteresis, before proceeding to a more accurate station-by-station analysis using available gaugings.

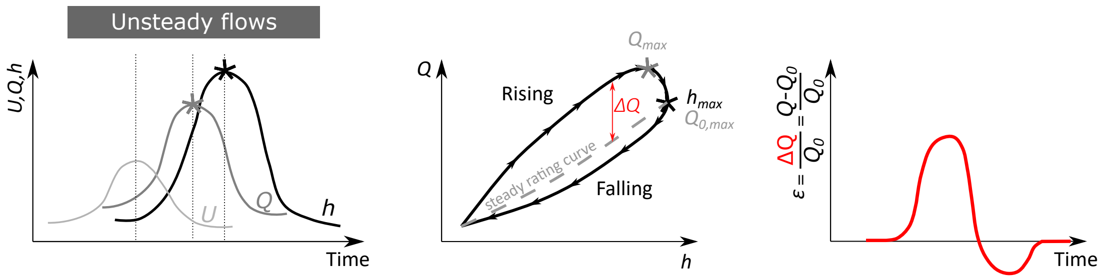

Figure 1: Discharge error due to flow unsteadiness hysteresis: temporal time series (U : average velocity, Q : discharge, h : stage), rating curves (dashed line for steady uniform flow regime and solid line for unsteady flow regime) and the relative discharge error ϵ comparing the two discharges of the two different regimes (Q: unsteady discharge, Q_0: steady discharge).

The rest of the paper is organized as follows. First, the rating curve model for unsteady flows used in the diagnosis procedure is detailed in Section 2. Simple rating curve models such as the well-accepted Jones (1915) equation are preferred for the diagnosis because it requires limited information that is available on large datasets and easily measurable on the field. The presented method is intended to be used for hydrometric purposes. Other more complex equations mentioned above require too much additional information and as shown by Mansanarez (2016), they do not significantly improved nor reduced the uncertainty related to the estimation of the discharge during unsteady flows compared to Jones (1915) equation. Then, the generic framework is described in Section 3 along with the required input data and the criteria retained for quantifying the hysteresis effect. The diagnosis is eventually applied to the gauging stations of the French national hydrometry network (Section 4). The limit of the method is pointed out using a sensitivity analysis of input data of the hysteresis model.

2 Theory

2.1 Rating curve model for steady uniform flow

Hysteresis due to transient flows is known to be observed during intense floods. In those conditions, it is usually relevant to approximate the hydraulic controls at gauging stations by a single channel control. The diagnosis is therefore performed with this assumption.

The Manning-Strickler equation is generally used for stage-discharge models of gauging stations with channel controls, for which the flow is mainly controlled by friction (Rantz, 1982; World Meteorological Organization, 2010; Le Coz et al., 2014) :

$$Q_0 \approx K A R_h^{2/3} \sqrt{S_0} \tag{1}$$

with Q_0 [m^3/s] the discharge in uniform steady flow, K [$m^{1/3}.s^{-1}$] the Strickler flow resistance coefficient, A [m^2] the wetted area, R_h [m] the hydraulic radius and S_0 [-] the channel slope. A unique relation between stage and discharge is thus obtained. Equation 1 is valid only for uniform steady flow; although it is often used for non-uniform unsteady flows in the hydraulic community.

2.2 Rating curve model for unsteady flow - Jones equation

Equation 1 is based on the assumption that the energy slope S_f can be approximated by the channel slope S_0. It is not applicable in case of unsteady flow. Indeed, the water free-surface varies continuously during the flood wave propagation and the longitudinal water profile is not parallel to the river bed profile. Therefore, a correction of the steady-flow rating curve is required to capture the hysteresis effect. The energy slope S_f can be expressed through the one-dimensional momentum equation of Saint-Venant, which describes the full dynamics of a flood wave propagation :

$$S_f = S_0 - \frac{\partial h}{\partial x} - \frac{1}{g}\left(\frac{\partial U}{\partial t} + U\frac{\partial U}{\partial x}\right) \tag{2}$$

with g [$m.s^{-2}$] the gravitational acceleration, U [$m.s^{-1}$] the cross-sectional average water velocity, t [s] the time, x [m] the streamwise distance and h [m] the water surface elevation (a.k.a. the stage). The relative importance of the terms detailing the full dynamics of the flood wave propagation (Equation 2) determines the type of wave occurring at specific sites and particular events (Muste et al., 2020). For example, neglecting the inertia terms compared to the pressure term and gravity force leads to the so-called diffusion wave (Equation 3):

$$S_f \approx S_0 - \frac{\partial h}{\partial x} \text{ (diffusion wave assumption)} \tag{3}$$

The diffusion wave assumption is generally accepted for low-gradient channels.

Combining Equation 1 and Equation 3, the stage-discharge model for unsteady flow becomes:

$$Q = Q_0 \sqrt{1 - \frac{1}{S_0} \frac{\partial h}{\partial x}} \tag{4}$$

The discharge is therefore expressed as a steady-flow reference discharge Q_0 multiplied by a corrective term accounting for flow unsteadiness.

The Jones (1915) approximation avoids estimating the longitudinal gradient term $\partial h/\partial x$, which is rarely measured at gauging stations, except in the case of twin gauge stations (Petersen-Øverleir and Reitan, 2009; Mansanarez, 2016). As a substitute, the temporal variation of stage $\partial h/\partial t$ is used, which is always available from stage records. The Jones approximation is based on the kinematic wave assumption, which assumes that the wave propagates with no attenuation along the channel. The flood wave celerity c can therefore be expressed as :

$$c = \frac{\partial x}{\partial t} = \frac{\partial Q}{\partial A} \tag{5}$$

Assuming a prismatic channel and vertical river banks over the range of stage variation, the flood wave celerity becomes:

$$c \approx \frac{1}{B} \frac{\partial Q_0}{\partial h} \tag{6}$$

where B [m] is the channel width.

The continuity equation of Saint Venant for quasi-steady flows can be rearranged to show the relationship between the longitudinal and temporal gradients (see Mansanarez (2016) for details):

$$\frac{\partial h}{\partial x} = -\frac{1}{c}\frac{\partial h}{\partial t} \tag{7}$$

With such approximation, the rating curve model can be expressed as follows, where S_f is expressed from the bed slope, the flood wave celerity and the stage time-gradient:

$$Q = Q_0\sqrt{1 + \frac{1}{cS_0}\frac{\partial h}{\partial t}} \tag{8}$$

Equation 8 is referred to as the Jones equation in the following.

In the rest of the paper, the channels at gauging stations are approximated by wide and rectangular channels with equivalent conveyance in order to perform the hysteresis diagnosis at large-scale with a minimum of information on the channel geometry. This assumption is acceptable in conditions of floods inducing hysteresis (Le Coz et al., 2014). Then, the hydraulic radius can be approximated by the flow depth : $R_h \approx (h - b)$, where b is the offset of the channel control. Equation 8 becomes:

$$Q = KB(h-b)^{5/3}\sqrt{S_0}\sqrt{1 + \frac{1}{\frac{5}{3}K(h-b)^{2/3}S_0^{3/2}}\frac{\partial h}{\partial t}} \tag{9}$$

2.3 Quantification of the hysteresis effect

The hysteresis effect is quantified based on the relative discharge error ϵ between the discharge calculated considering the flow as unsteady (Q) and the discharge calculated assuming a steady flow regime (Q_0). Combining Equations 1 and 9, ϵ is expressed as follows :

$$\epsilon = \frac{Q - Q_0}{Q_0} = \sqrt{1 + \frac{1}{\frac{5}{3}K(h-b)^{2/3}S_0^{3/2}}\frac{\partial h}{\partial t}} - 1 \tag{10}$$

Analysing Equation 10, the main requirements for detecting stations with hysteresis due to flow unsteadiness are : 1) low S_0, 2) high stage temporal gradients $\partial h/\partial t$ (i.e. stations subject to intense and rapid floods), and 3) rough beds inducing high flow resistances (i.e. low K).

Assuming that $\epsilon << 1$ and after a first-order Taylor expansion, Equation 10 can be rearranged as follows :

$$\epsilon \approx 0.3K^{-1}(h-b)^{-2/3}S_0^{-3/2}\frac{\partial h}{\partial t} \tag{11}$$

To investigate the relative importance of the different factors of Equation 11 in this hysteresis phenomena, i.e. K, S_0, $(h-b)$ and $\partial h/\partial t$, the relative uncertainty of ϵ is assessed applying the uncertainty propagation law of JCGM (2008) (Joint Committee for Guides in Metrology) to Equation 11 and assuming independent measurement errors :

$$u_\epsilon'^2 = u_K'^2 + \frac{4}{9}u_{(h-b)}'^2 + \frac{9}{4}u_{S_0}'^2 + u_{\partial h/\partial t}'^2 \tag{12}$$

where $u'_X = u_X/X$ is the relative standard uncertainty of the variable X. The sensitivity coefficients in Equation 12 inform about the relative importance of each factor for the hysteresis effect quantification. The bed slope is the most sensitive parameter, with a sensitivity coefficient of 9/4. To a lesser extent, K and $\partial h/\partial t$ are also important; they have a sensitivy coefficient equal to 1. Equation 12 indicates that $(h-b)$ is the less sensitive factor, with a sensitivity coefficient of 4/9.

3 The diagnostic approach

3.1 Required data

The diagnosis consists in applying Equation 10 to each hydrometric station, which requires estimates of the flow resistance coefficient K, the bed slope S_0, the bed elevation b, the stage time series and the time-gradient $\partial h/\partial t$. Figure 2 illustrates the different steps to follow to collect the needed data for each gauging station. The diagnosis can be easily re-applied as more input data are available.

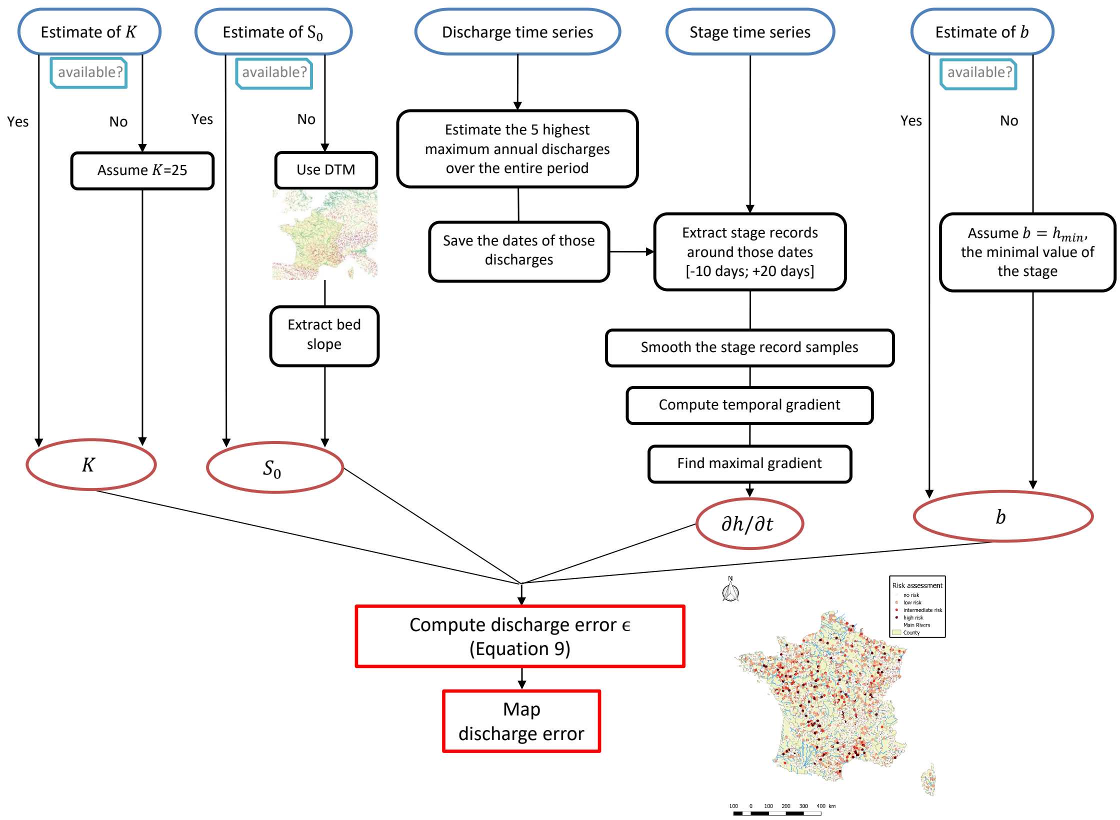

Figure 2: The framework for diagnosing gauging stations influenced by hysteresis effect due to flow unsteadiness.

The flow resistance coefficient K (or the Manning's coefficient $n = 1/K$) is generally not documented in national databases. It might be possible to retrieve this information for specific stations from local hydrological services but this is rarely available. As indicated in Figure 2, if not available, defaults values for K need to be assumed. The analysis of Equation 11 showed that discharge error is inversely proportional to K. It is therefore more likely to observe hysteresis at stations with low K values, i.e. rough beds. If no estimate of K is available, we set $K = 25$ as a conservative but realistic default value. A flow resistance coefficient of 25 represents rough gravel-beds, or beds with bedforms or presence of vegetation (Coon, 1998).

An accurate measure or evaluation of the bed slope S_0 is crucial for a good performance of the method (see Equation 12). It may be available at some gauging stations from hydraulic studies or specific topographic surveys. But over a national network, we need to use S_0 estimates from external datasets, e.g. based on Digital Terrain Models (DTM).

The time-gradient $\partial h/\partial t$ is estimated based on the stage time series $h(t)$ that are automatically and continuously recorded at gauging stations (cf. Figure 2). Those records are then registered in large databases and converted into discharge time series $Q(t)$ using rating curves established from discharge measurements (gaugings) at the stations. The higher gradients $\partial h/\partial t$ are assumed to be found during the most intense floods. The method scans the data to estimate the largest five time-gradients $\partial h/\partial t$ for each specific station. First, the largest five flood peaks are detected from the discharge time series $Q(t)$ for each station over the entire period of available data. Samples of stage time series $h(t)$ are extracted around those extreme events. Data starting 10 days before the flood peak to 20 days after are kept. This duration was defined assuming it was sufficient to capture the flood dynamics at all stations. The resulting stage data are smoothed using a spline function to remove noise and keep only the stage variations reflecting the flood propagation. When the amount of missing data within the recorded stage time series is too large, it is excluded from the diagnosis. The gradient $\partial h/\partial t$ time series are then calculated from the smoothed $h(t)$ and the five maximum values of the gradient over the five events are kept for computing ϵ.

It is difficult to set the offset b of the channel control, mostly because it can evolve due to erosion/deposition, and in particular after floods inducing large sediment transport. As a consequence, b is seldom recorded in databases. If not available, we suggest setting $b = h_{min}$ in the framework, where h_{min} corresponds to the lowest stage value of the stage time series of the studied event. Indeed, the cease-to-flow level b of the channel should not be higher than the lowest stage recorded.

3.2 Mapping hysteresis effect

Once the parameters K, b, h, S_0 and $\partial h/\partial t$ are identified (see Section 3.1), the discharge error can be computed using Equation 10. The procedure gives five estimates of ϵ for each stations, because the greatest five flood events are analysed (Figure 2).

The hysteresis effect is qualitatively assessed based on the resulting ϵ that we choose to present and map in two ways. Firstly, the focus is made on the most critical event per stations inducing the higher relative error ϵ_{max}. The maximal discharge errors ϵ_{max} are mapped by classes to facilitate the qualitative assessment. Four classes are chosen according to usual criteria in hydrometry accounting for the uncertainties of the rating curves and gaugings : 1) negligible deviation between Q and Q_0 (i.e. $\epsilon_{max} \leq 1\%$), 2) low deviation (i.e. $1\% < \epsilon_{max} \leq 5\%$), 3) intermediate deviation (i.e. $5\% < \epsilon_{max} \leq 10\%$), and 4) high deviation (i.e. $\epsilon_{max} > 10\%$), i.e. larger than typical gauging uncertainties, which are generally evaluated to range 7-10% depending on the measurement technique. Secondly, the hysteresis effect can be assessed for each station by the number n_ϵ representing the number of floods over the selected five for which the discharge error is larger than an arbitrary threshold, set as 10% in our application. The indicator n_ϵ is divided into three classes to facilitate the hysteresis assessment using the map: 0 - station not prone to hysteresis, 1 - station with low exposure to this effect, from 2 to 5 - station prone to hysteresis effect.

The first map produces a general diagnosis and enables to detect all the potentially affected stations. The second map is complementary and gives a refined diagnosis showing the stations that are frequently affected by hysteresis. Those maps can be used as a guide for hydrological services to identify the affected stations and to better manage their stations. The thresholds for the assessment of hysteresis influence can be reviewed to match the requirements of each hydrological service.

4 Application to France's national hydrometry network

4.1 Presentation of the data

The framework is applied to France's national hydrometry network. A number of 2618 gauging stations are analysed, which corresponds to stations with discharge rating (not stage only), including closed or discontinued stations. The stage and discharge times series required for the method to work come from the national hydrological archive (HYDRO2 database). Estimates for K, b, and S_0 are not available in HYDRO2 database. The flow resistance coefficient was assumed equal to 25 for all the stations as a conservative assumption. Approximates of channel bed slopes are deduced from three datasets using different DTMs for slope extraction with different resolutions and spatial coverages (Figure 3) :

1. the Global River Slope dataset, GloRS (Figure 3a), which is a worldwide geospatial dataset detailed in Cohen et al. (2018), where the slope is simply calculated from the elevation depression over the length of a river reach. The slope extraction is made based on the 15arc-sec resolution ($\sim 460\times460$ m) SHuttle Elevation Derivatives at multiple Scales (HydroSHEDS) DTM and stream-network (see `http://hydrosheds.cr.usgs.gov/index.php`). The reaches are defined according to the confluence points and to an additional feature-splitting procedure, which splits the river segments that are longer than a user-defined distance. A 50-km splitting interval was selected in Cohen et al. (2018), as it exhibits the best correlations to their validation dataset. The reach lengths vary from 156 m to 50 km with a mean length of $\sim$17 km in the world dataset. The smallest reach slope detected is 5.3×10^{-5}; smaller slopes are set to 0. In France, a specific correspondence is made between the reach and the location of the gauging station on the basis of the closest distance between both objects. The station slope is then set equal to the slope of the associated reach. If the distance exceeds 200 m between station and reach, the

station is excluded. In France, the smallest slope is 2.5×10^{-4}.

2. the theoretical hydrographical network (RHT) (Pella et al., 2012) (Figure 3b), which is a joined and oriented digital river network (see `https://ecoflows.inrae.fr/software/`). It is derived from the BD Alti® 50 m digital elevation model of the French Geographic National Institute (IGN) and from the extended hydrological network (RHE) (Pella et al., 2008) corresponding to an oriented simplification of the referential hydrographical network of the IGN, BD Carthage®. The final RHT represents a network of 283 639 km with a total of 114 601 reaches associated with different topographic, climatic and hydrologic attributes. Various environmental attributes are available and presented in Pella et al. (2012), such as slope estimates, catchment areas, mean discharge, reach width and length for example. The slope is calculated as the difference in elevation between the upstream and downstream ends of the reach divided by the reach length. The lowest reach slope detected in the RHT is equal to 10^{-4}; smaller slopes are set to 0. The average reach length is 2.5 km and varies from a few meters to more than 40 km. The reach-station association is made by geographical proximity. On average, the distance between the two objects does not exceed 36 m.

3. the slopes from the hydrological distributed model J2000-Rhône (Branger et al., 2018) (Figure 3c), covering the Rhône River basin (97 800 km^2), located Southeast of France. The tool called HRU-delin (Hydrological Response Unit - delineation) combined with a DTM is used to prepare the mesh and generate several inputs for the hydrological modeling, including the creation of river reaches and calculation of their slopes (see `https://forge.irstea.fr/projects/hru-delin`). The slope dataset results from the SRTM (Shuttle Radar Topographic Mission) digital elevation data, with a resolution of 90 m. The reach lengths are defined by the confluences and the locations of the gauging stations, hence a wide range of lengths, from 90 m to more than 44 km with a mean length of ∼6 km. The slopes are extracted for each reach by

computing the difference in altitude between the upstream and downstream pixel of the reach. The minimum slope detected in the dataset is equal to 8.3×10^{-5}; smaller slopes are set to 0. A specific correspondence is made between the reach and the location of the gauging station to obtain the S_0 value at the station. The stations are first relocated on the stream network by proximity and similarity of drainage area. The reaches are then cut at the station position on the stream, so that the end of the reach corresponds to the station location.

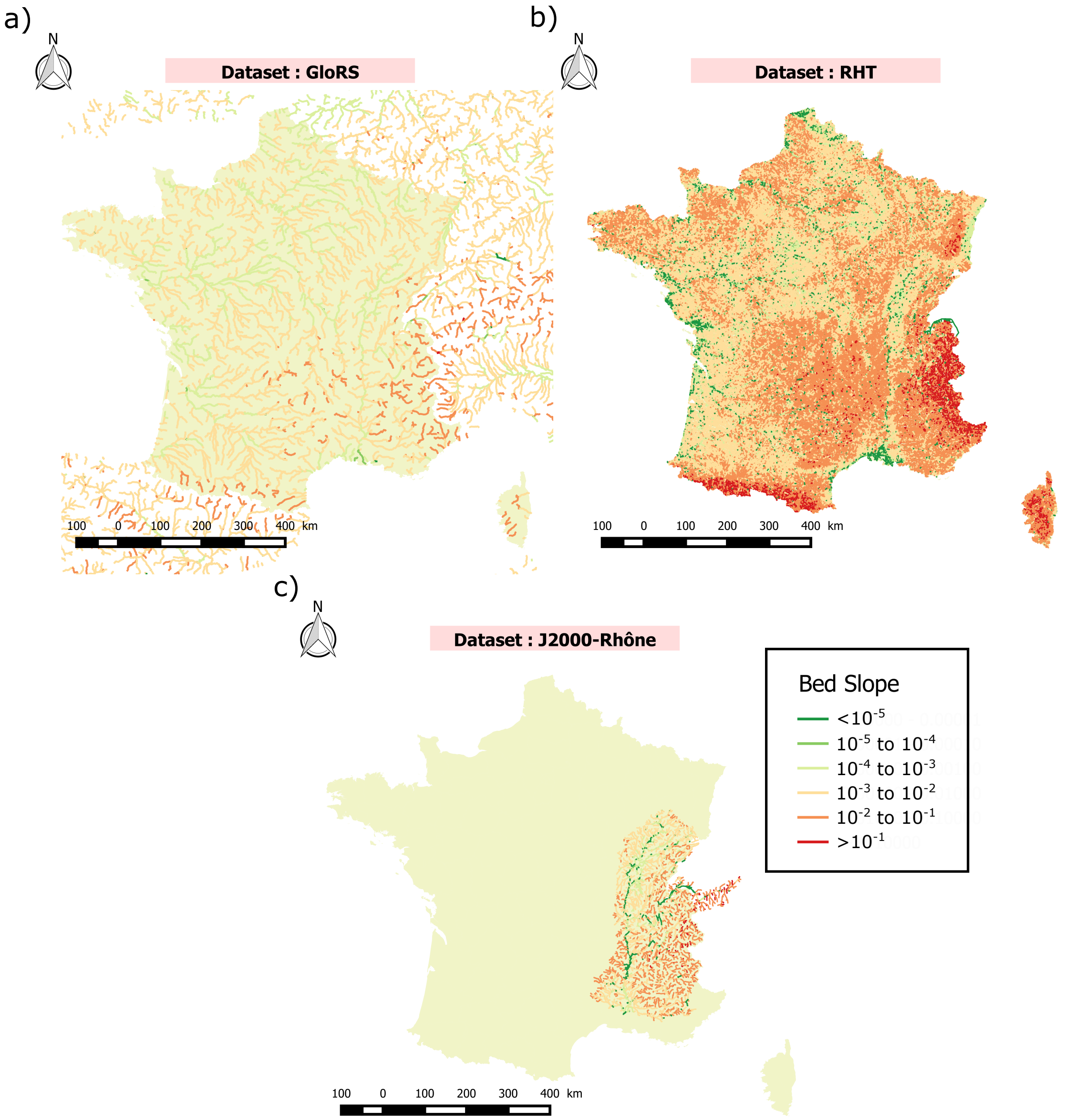

Figure 3: River slope estimates in France from different datasets : a) GloRS, b) RHT and c) J2000-Rhône.

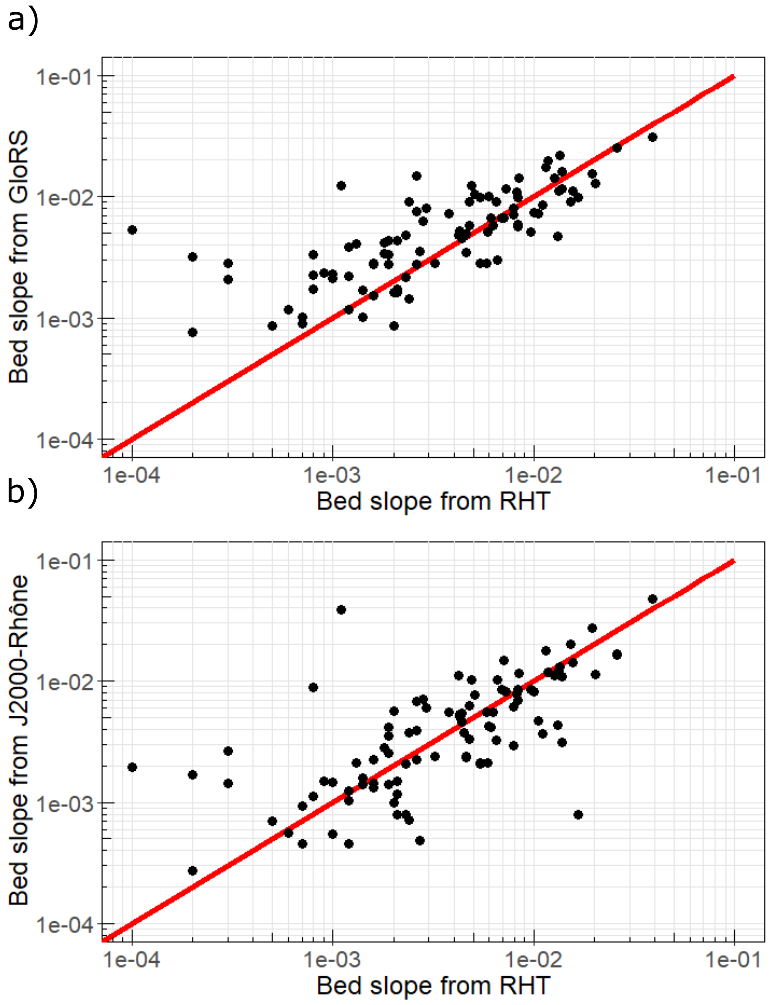

Figure 4: Comparison of bed slope estimates obtained after extractions from different datasets for 99 gauging stations located in the Rhône basin: a) bed slopes from GloRS versus from RHT, and b) bed slopes from J2000-Rhône versus from RHT.

The GloRS provides slope estimates only for the main rivers, whereas the two other datasets also include S_0 estimates for small rivers and headwater catchments. The values of S_0 differ according to the chosen dataset, but the same general trend is observed, i.e. high and low slopes are detected approximately in the same areas (Figure 3). The slope estimates can vary for more than one magnitude order (Figure 4). Slopes from RHT and J2000 are in closer agreement than slopes from GloRS, which might be explained by differences in the DTM resolution.

4.2 Results over France

The diagnostic maps for France's national hydrometry network differ according to the chosen source of S_0 estimates (Figure 5). Slope estimates were available for the 2618 gauging stations using the RHT dataset whereas the GloRS and J2000-Rhône datasets provide slope estimates for only 1053 and 298 gauging stations, respectively. The smallest French rivers are not represented in GloRS dataset, leaving some gauging stations without a slope estimation during the reach-station matching. The diagnostic maps based on the RHT and J2000-Rhône slope estimates reflect what was initially expected : a greater risk of hysteresis near estuaries (e.g. estuary of the Rhône River) and on large rivers with low-gradient slopes (e.g. Saône River); see Figure 5d. In addition, stations located in mountains (e.g. Alps) are identified as not prone to hysteresis effect.

According to the diagnosis, 186 out of 2618 stations (i.e. 7.1%) are prone to substantial hysteresis effect (ϵ >10%) based on S_0 estimates from the RHT (Figure 6a), whereas only 29 stations out of 1053 (i.e. 2.8%) are prone to hysteresis based on S_0 estimates from the GloRS (Figure 6b). Even if the diagnostic results are different, we can safely say that the hysteresis effect is low in France. Note that some low-gradient stations prone to hysteresis might have been missed because their slopes were lower than the threshold value imposed by the used datasets. In addition, further investigation is required to conclude if the detected stations are really prone to hysteresis, such as a specific analysis of gaugings and rating curves at individual stations.

4.3 Profiles of stations prone to hysteresis

The framework results can be used to determine the typical profile of stations prone to hysteresis. Figure 7 presents the needed geometrical and hydraulic conditions (i.e S_0 and $\partial h/\partial t$) to observe hysteresis at a station. As expected, low bed slope combined with high temporal stage variation are the critical conditions. This is in accordance with the uncertainty analysis made for Equation 10. As shown in

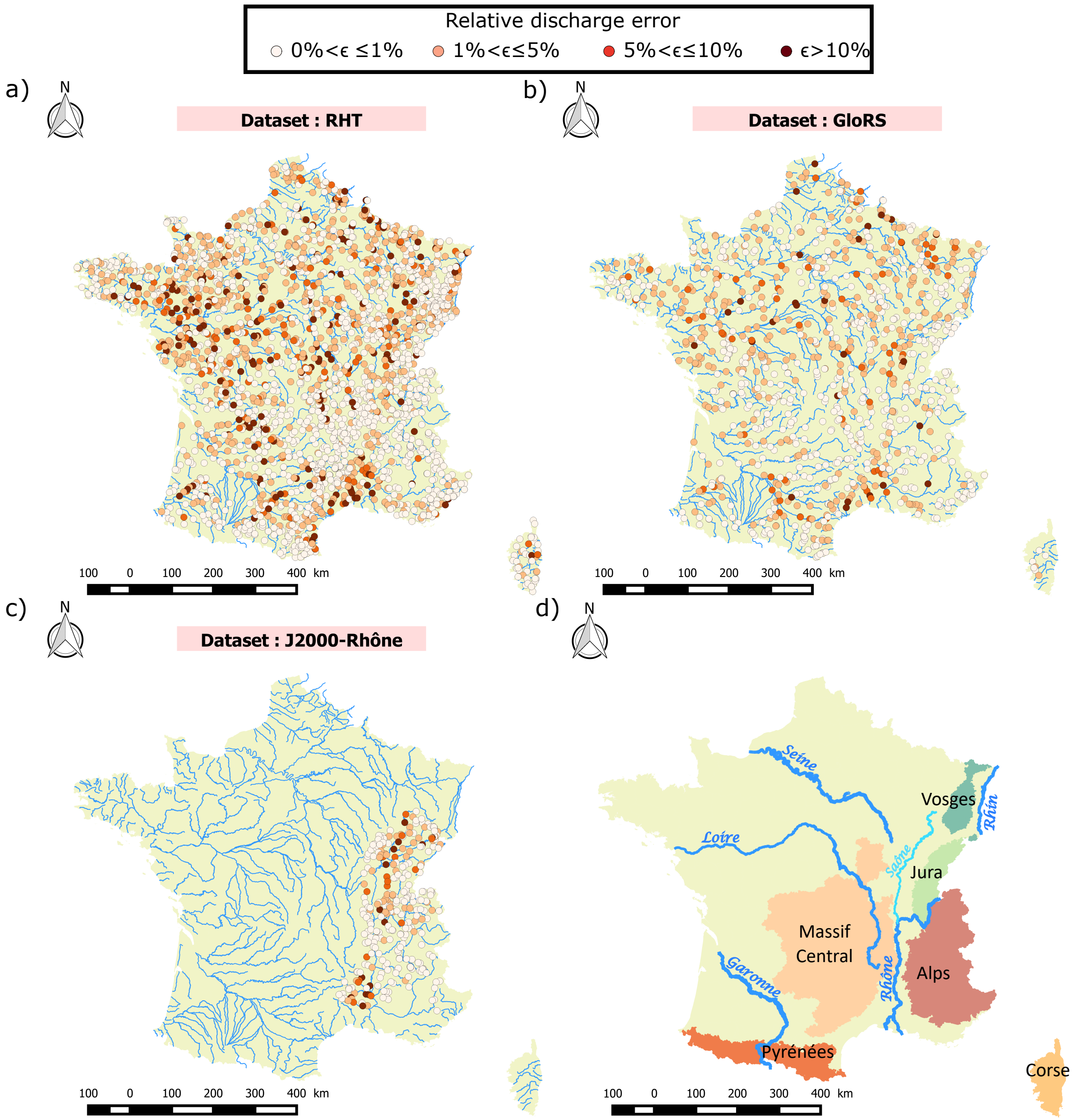

Figure 5: Diagnostic maps of hysteresis influence on 2618, 1053 or 298 gauging stations in France, using a) RHT, b) GloRS or c) J2000-Rhône dataset as input data for river bed slope, respectively. d) Overview of the main rivers and mountains in France.

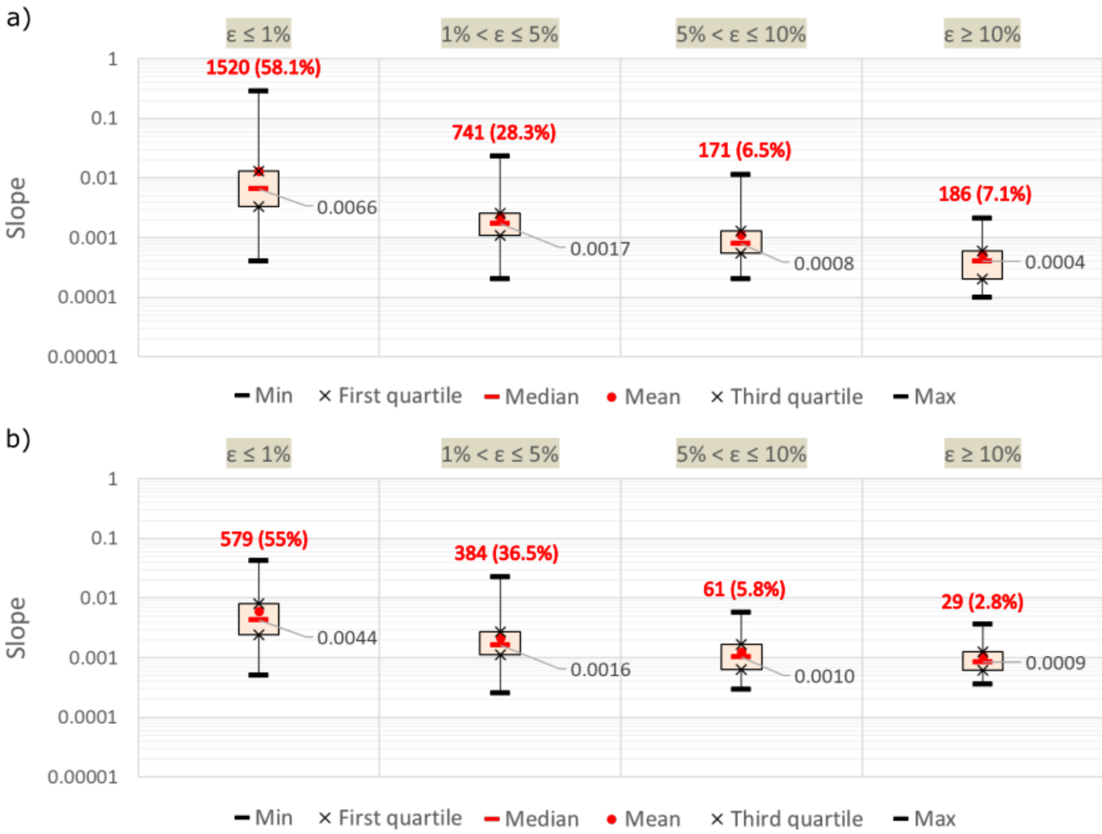

Figure 6: Relationship between classes of relative errors due to hysteresis effect ϵ and bed slopes S_0 deduced from a) the RHT and b) from the GloRS datasets. The red numbers indicate the number of stations within the class and the percentage with respect to the total number of stations, respectively.

Figures 6 and 7, stations with high relative discharge errors ($\epsilon > 10\%$) have low bed slopes varying mainly from 10^{-4} to 10^{-3} and high time stage gradient ranging from 4×10^{-6} to 10^{-3}m/s. Those values are in accordance with typical values reported in the literature and listed by Muste et al. (2020). Hysteresis is generally considered negligible when $S_0 > 10^{-3}$ and $0 < dh/dt < 3.3 \times 10^{-4}$m/s and becomes clearly significant when $S_0 < 10^{-4}$ and $dh/dt > 4.2 \times 10^{-6}$m/s (Fread, 1975; Muste et al., 2020), as observed in Figure 7. Unfortunately, we have limited estimates of S_0 smaller than the lower slope threshold of 10^{-4}.

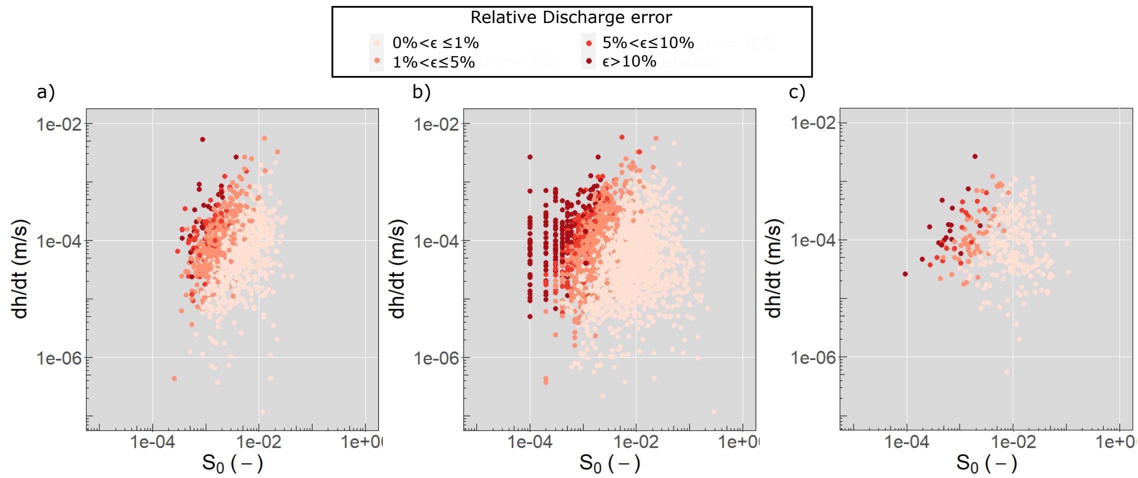

Figure 7: Stage temporal variation $\partial h/\partial t$ versus bed slope estimates S_0 deduced from a) GloRS, b) RHT and c) J2000-Rhône datasets for the different gauging stations and associated assessment for hysteresis effect ϵ.

4.4 Sensitivity to slope data

Testing diverse sources of bed slope data enables to evaluate the sensitivity of the diagnosis to those input data. The application over the Rhône basin using the J2000-Rhône data stresses the importance of using such accurate estimates of bed river slopes. Figure 8 shows the three diagnostic maps for the 99 stations shared by the three datasets in the Rhône basin. If the GloRS slope dataset is used as input, no stations are detected as prone to hysteresis; the relative discharge error ϵ being always lower than $\sim$8% (see Figure 9a). Conclusions are significantly different if RHT or J2000-Rhône slope datasets are used. Only 6 and 7 stations are affected by hysteresis according to the diagnosis made with S_0 estimates from RHT and J2000-Rhône datasets, respectively. Two of these stations are common to the two datasets.

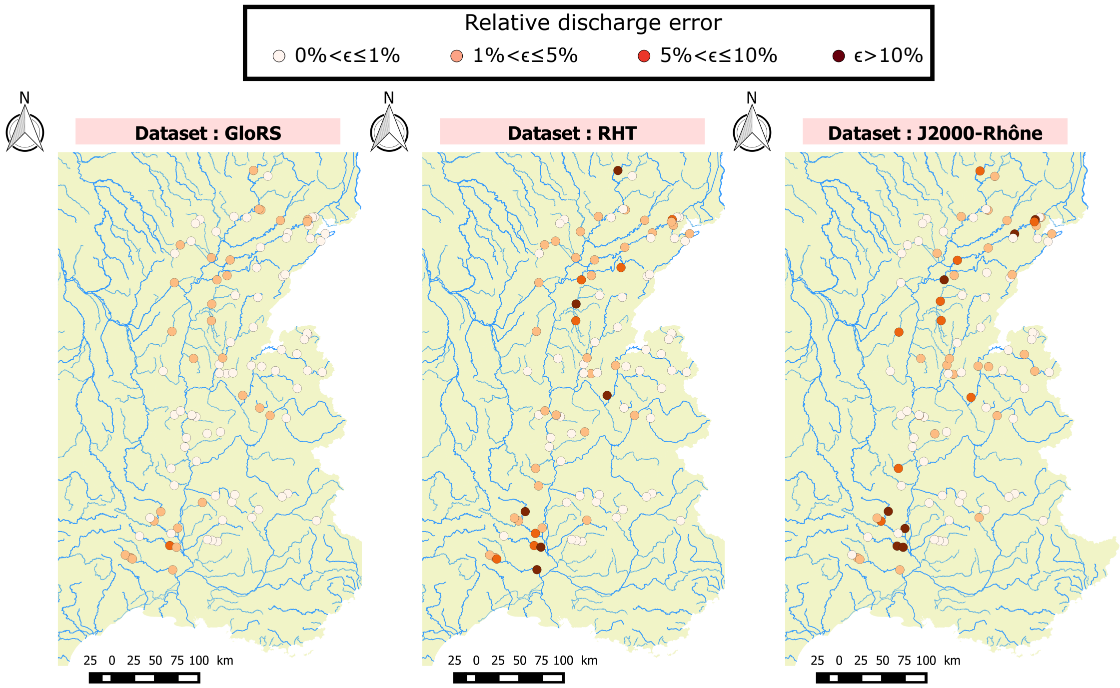

Figure 8: Diagnostic maps of hysteresis influence on the 99 gauging stations located in the Rhône basin, France, using slopes estimated from different DTM: GloRS, RHT and J2000-Rhône.

The resulting discharge errors highly depend on the S_0 estimates used for their computation. The discharge errors calculated using the GloRS slope dataset are mostly underestimated compared to those calculated using the RHT slope dataset (see regression line in Figure 9a). There is no obvious bias between ϵ deduced from RHT and J2000-Rhône slope datasets. A large scatter of ϵ values is nevertheless observed in Figure 9b. The high values of ϵ are realistic, in particular those calculated using J2000-Rhône slope estimates; in that case ϵ does not exceed 48% (Figure 9b). Only one station out of the 99 stations in the Rhône basin has a discharge error that exceeds 100% (ϵ=445% according to the diagnosis made with the RHT slope dataset). For clarity, this point is not presented in Figure 9. This station is also identified as prone to hysteresis by the diagnosis deduced from the J2000-Rhône slope dataset ($\epsilon \approx$15%). The out of range value is probably the consequence of a wrong S_0 estimate. Indeed, S_0 differs by more than one order of magnitude compared to S_0 from J2000-Rhône and GloRS datasets. In addition, the consistency of the other input data such as the time stage gradient was verified. Regarding the entire France network, there is only 15 out of 2618 stations (less than 0.6%) with a discharge error higher than 100% and all of these ϵ result from an estimation based on RHT slope dataset. This is encouraging with regard to the use of such a diagnostic approach.

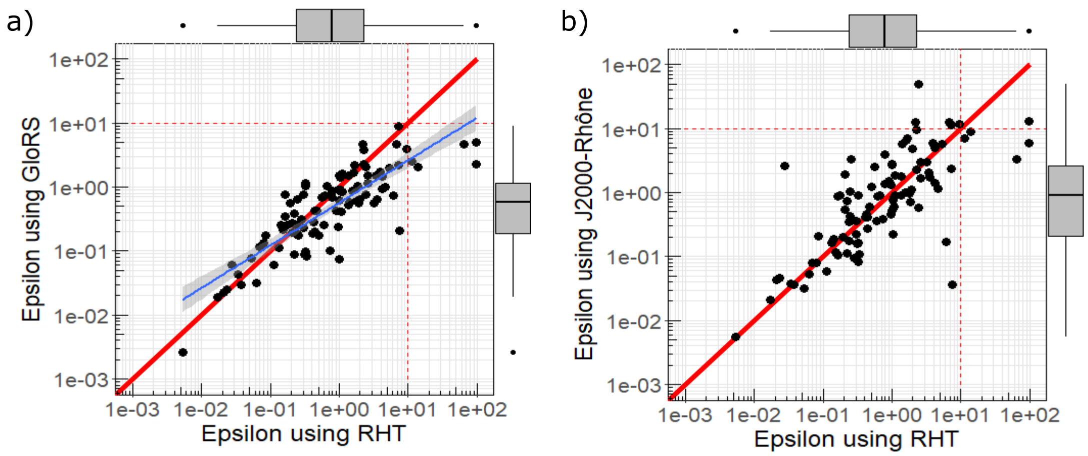

Figure 9: Comparison of discharge errors ϵ calculated using the slope estimates from different datasets for 99 gauging stations located in the Rhône basin: a) using GloRS versus RHT, and b) using J2000-Rhône versus RHT. Marginal boxplots detail the distribution of the data. Red solid and dotted lines represent the perfect agreement and the threshold of $\epsilon = 10\%$, respectively. Blue line refers to a linear regression line with its grey envelop corresponding to the confidence interval.

4.5 Limit of the diagnostic approach

The main limit of the proposed framework is therefore related to the difficulty to estimate the bed slope massively and accurately. Slope calculation is scale-dependent and is thus sensitive to the spatial resolution of the DTM as well as the reach length. The key to have a good diagnostic performance is to use local estimation of bed slope. In the best case scenario, the slope should be evaluated over the length where the channel characteristics control the stage-discharge relation, but such a length is hard to identify and especially is site-specific. Such diagnosis is thus challenging, because we need to perform a diagnosis at large-scale (e.g. over country) of individual local objects (stations). No dataset at the local scale for the slope estimates exists, so we extract them from large-scale datasets that were not developed for local studies. The splitting procedure for the reaches in the datasets is most often not suitable for our purpose, though accurate for hydrological studies. The reach length is often too long to capture the accurate value of the bed slope at the station. For example, the average reach length associated to the 1053 stations in the GloRS dataset is 27 km, whereas it is equal to 4 km and 6.1 km, for the 2618 and 298 stations in the RHT and J2000-Rhône datasets, respectively. Using such input data in the framework gives nonetheless a good overview of the global dynamics around the station in conditions of intense floods. In our framework, we mix data from different scales: averaged bed slopes over variable-length reach and local information at the station such as, the stage time series and geometrical characteristics. If there is any doubt about the value of ϵ at a specific station, we recommend measuring directly and locally the river bed slope around the station. The discharge error can then be re-calculated with good S_0 estimate. If the station is detected as prone to hysteresis effect, an adjusted stage-discharge relation should be used for discharge prediction rather than the standard rating curve, such as for example Equation 8, or variant models as those reported in Petersen-Overleir (2006); Mansanarez (2016).

5 Conclusion

A diagnostic method is proposed to detect the gauging stations prone to hysteresis due to flow unsteadiness over a given hydrometry network. It uses well-known hydraulic concepts related to unsteady flows, such as the Jones equation, and simple data, i.e. easily measurable or estimable parameters on the field, such as those generally present in national hydrological databases. The final output is a map assessing the hysteresis effect at all the stations from the studied area through the relative discharge error between the discharge calculated with the steady flow rating curve and the actual discharge. The application of the method to France's national hydrometry network highlights the importance of using reliable bed slope estimates to produce a robust diagnosis. The major limit of the method is to have access to accurate local bed slopes. The diagnostic maps obtained using three different inputs of bed slope estimates show that in France the hysteresis effect due to flow unsteadiness is low for the majority of the gauging stations; 7.1% of the 2618 gauging stations are potentially affected by hysteresis according to the diagnosis made with the slope estimates from RHT dataset. However, the diagnostic results differ depending on the source (and accuracy) of the slope estimates. In the future, particular attention should be paid to measuring accurately the river bed slopes near the gauging stations and therefore refining the rating curves in case of unsteady flows with specific gauging campaigns.

Acknowledgements

This work was funded by the SCHAPI, France's national hydrological service (SRNH 2018 and 2019 contracts about natural risks between INRAE and the Ministry of Ecology). The authors would like to gratefully thank Benjamin Renard (INRAE) for his contribution to the method development and for all the interesting discussions we had about the hysteresis subject. We also thank Flora Branger (INRAE) and Hervé Pella (INRAE) for their help for collecting the bed slope data from the J2000-Rhône model and the RHT, respectively.

Competing interests

The authors declare that they have no competing interests.

References

Boyer, M. (1964). *Streamflow measurement (chapter 15) in Handbook of Applied Hydrology.* McGraw-Hill.

Branger, F., Gouttevin, I., Tilmant, F., Cipriani, T., Barachet, C., Montginoul, M., Le Gros, C., Sauquet, E., Braud, I., and Leblois, E. (2018). A distributed hydrological model to assess the impact of global change on water resources in the Rhône catchment. In *IS Rivers*, Lyon, France.

Cohen, S., Wan, T., Tasmul Islam, M., and Syvitski, J. (2018). Global river slope: a new geospatial dataset and global-scale analysis. *Journal of Hydrology*, 563:1057–1067.

Coon, W. (1998). Estimation of roughness coefficients for natural stream channels with vegetated banks. *U.S. Geological Survey Water Supply*, Paper 244:145.

Dottori, F., Martina, M., and Todini, E. (2009). A dynamic rating curve approach to indirect discharge measurement. *Hydrology and Earth System Sciences*, (13):847–863.

Dramais, G., Le Coz, J., Hauet, A., and Camenen, B. (2011). Advantages of a mobile LSPIV method for measuring flood discharges and improving stage-discharge curves. *Journal of Hydro-Environment Research*, 5(4):301–312.

Fenton, J. and Keller, R. (2001). The calculation of streamflow from measurements of stage. Technical report, Cooperative research center for catchment hydrology, Melbourne, Australia.

Fread, D. (1975). Computation of stage-discharge relationship affected by unsteady flow. *Water Resources Bulletin*, 11(2).

Graf, W. H. and Qu, Z. (2004). Flood hydrographs in open channels. *Proceedings of the Institution of Civil Engineers - Water Management*, 157(1):45–52.

Holmes, R. (2016). River rating complexity. In Constantinescu, G. and Hanes, editors, *International Conference on Fluvial Hydraulics (River flow 2016)*. Taylor & Francis Group.

JCGM (2008). Evaluation of measurement data - guide to the expression of uncertainty in measurement. Technical Report Guide 100.

Jones, B. E. (1915). A method of correcting river discharge for a changing stage. *U.S. Geological Survey Water Supply*, (375-E):117–130.

Le Coz, J., Renard, B., Bonnifait, L., Branger, F., and Le Boursicaud, R. (2014). Combining hydraulic knowledge and uncertain gaugings in the estimation of hydrometric rating curves: A Bayesian approach. *Journal of Hydrology*, 509:573–587.

Lee, K. (2013). *Evaluation of methodologies for continuous discharge monitoring in unsteady open-channel flows*. PhD thesis, The University of Iowa.

Lee, K. and Muste, M. (2017). Refinement of the fread method for improved tracking of stream discharges during unsteady flows. *Journal of Hydraulic Engineering*, 143(6).

Mansanarez, V. (2016). *Non-unique stage-discharge relations: Bayesian analysis of complex rating curves and their uncertainties*. PhD thesis, Université Grenoble Alpes.

Muste, M., Lee, K., Kim, D., Bacotiu, C., Oliveros, M., Cheng, Z., and Quintero, F. (2020). Revisiting hysteresis of flow variables in monitoring unsteady streamflows. *Journal of Hydraulic Research*, 58(6):867–887.

Pella, H., Lejot, J., Lamourous, N., and Snelder, T. (2012). Le réseau hydrographique théorique (RHT) français et ses attributs environnementaux. *Géomorphologie : relief, processus, environnement*, 3:317–336.

Pella, H., Snelder, T., Lamouroux, N., Vanderbecq, U., Shankar, U., and Rogers, C. (2008). Réseau hydrographique naturel étendu (RHE) construit à partir de la BD Carthage. *Ingénieries eau-agriculture-territoires*, (55-56):15–28.

Perumal, M., Shrestha, K., and Chaube, U. (2004). Reproduction of hysteresis in rating curves. *Journal of hydraulic engineering*, 130(9):870–878.

Petersen-Overleir, A. (2006). Modelling stage-discharge relationships affected by hysteresis using the Jones formula and nonlinear regression. *Hydrological Sciences Journal*, 51(3):365–388.

Petersen-Øverleir, A. and Reitan, T. (2009). Bayesian analysis of stage-fall-discharge models for gauging stations affected by variable backwater. *Hydrological Processes*, 23(21):3057–3074.

Rantz, S. E. (1982). Measurement and computation of streamflow: Volume 2. Computation of discharge. Technical report, USGS.

Welber, M., Le Coz, J., Laronne, J., Zolezzi, G., and Zamler, D. (2016). Field assessment of noncontact stream gauging using portable surface velocity radars (SVR). *Water Resources Research*, 52(2):1108–1126.

Wolfs, V. and Willems, P. (2014). Development of discharge-stage curves affected by hysteresis using time varying models, model trees and neural networks. *Environmental modelling & Software*, 55:107–119.

World Meteorological Organization (2010). Manual on Stream Gauging. Computation of discharge - Vol. II. Technical Report 1044, WMO.